Stability Analysis of Micropower Network

Sudip K. Mazumder, *Fellow, IEEE*, and Eduardo Pilo de la Fuente, *Senior Member, IEEE*

***Abstract*— Stability analysis of micropower networks is gaining importance given the dwindling gap of power generation and demand as well as increasing penetration of intermittent renewable energy sources. Instead of using prevalent small-signal analysis-based approaches, with predictions typically limited to the vicinity of the equilibrium, the outlined approach provides a sense of global/semiglobal stability. With regard to the latter, current approaches to stability analysis are primarily based on time-domain-, energy-function-, and common-Lyapunov-function-based analyses. This paper outlines a stability analysis approach based on polynomial Lyapunov function, which is determined algorithmically using sum-of-squares optimization in order to maximize the region of attraction (ROA) of an equilibrium solution. This procedure precludes the need for prior knowledge of the form of the Lyapunov or energy function. In this paper, the tradeoff between accuracy of determining the ROA of a power-system model and the computation overhead incurred is evaluated.**

***Index Terms*— Micropower network, optimization, polynomial Lyapunov function (PLF), stability analysis.**

I. Introduction

A STABILITY-ANALYSIS tool investigates the dynamic behavior of a micropower network following a destabilizing event and/or disturbance in the system. The primary objective of the stability analysis is to address the evolving behavioral dynamics involving the electrical distribution network, electrical loads, and the generators. In typical small-signal analysis [1], [2], the stability of equilibrium solution of the overall nonlinear power network model is obtained by linearizing the nonlinear model. The validity of the linearized (small-signal) model is near a small vicinity of the equilibrium solution, and hence using this model, the behavioral dynamics of the original system in the presence of large-signal response is not possible to carry out [3], [4]. In order to prove the large-signal stability of a micropower network [5], [6], a Lyapunov function (LF) $V(x)$ has to be found that fulfills the Lyapunov conditions in a domain Ω around the equilibrium point (located at $x = 0$, where x is the state variable vector) [7], [8]

$$\begin{cases} V(x) > 0 \text{ for } \forall x \neq 0 \\ V(0) = 0 \end{cases} \tag{1}$$

$$\dot{V}(x) = \nabla V(x) \cdot F(x) \leq 0 \text{ for } \forall x \tag{2}$$

where $F(x)$ are the functions of the differential equations of the analyzed system

$$\dot{x} = F(x). \tag{3}$$

In addition to assessing the stability of the system, from a practical point of view, it is useful to determine the region of attraction (ROA) of the equilibrium point(s) x_{eq} to assess robustness. Conceptually, the ROA of an equilibrium state x_{eq} is the set of all the states x from which the network evolves to the equilibrium point x_{eq} without quitting the ROA itself. Mathematically, the ROA can be defined [7] as a compact invariant set, connected to the equilibrium state x_{eq} defined by

$$V(x) < \gamma \quad \forall x \in \text{ROA}. \tag{4}$$

Once the LF and the value γ have been obtained, the stability in a state x of the system can be assessed simply by checking if $V(x) < \gamma$, which requires a considerably faster evaluation than other analysis methods. The first objective of this paper is to evaluate the feasibility of applying sum-of-squares (SOS) optimization [9], [10] techniques to determine a polynomial LF (PLF) in micropower-network stability problems. Once the feasibility has been determined, a second objective of this paper is to determine the ROA estimate of the equilibrium. A final objective is to assess the validity of the stability predictions (i.e., the ROA) obtained using the PLF with that obtained using time-domain simulation (TDS).

II. Synthesis of Polynomial Lyapunov Function

The stability of a system would be demonstrated just by identifying an LF satisfying (1)–(4) in a specific domain. However, as shown in Fig. 1, each LF leads to a different estimation of the ROA. Because the goal is to obtain the best possible estimation of the ROA, optimization techniques have to be used to determine the best LF (i.e., the LF leading to the widest estimate of the ROA). To force $V(x)$ to fulfill the Lyapunov conditions in the widest possible domain, a set containment problem is formulated with the following three different sets (as shown in Fig. 2).

1) *Set A (Green):* Set of the states x within an arbitrary radius β [in other words, satisfying the inequality $p(x) < \beta$, where $p(x)$ has an arbitrary shape].

Manuscript received February 19, 2016; revised June 13, 2016; accepted July 8, 2016. This work was supported in part by the U.S. Department of Energy under Grant DE-OE00000625 and in part by the U.S. National Science Foundation under Grant 1239118. Recommended for publication by Associate Editor Riming Shao.

S. K. Mazumder is with the University of Illinois at Chicago, Chicago, IL 60607 USA (e-mail: mazumder@uic.edu).

E. Pilo de la Fuente is with EPRail Research and Consulting, Madrid 28049, Spain (e-mail: eduardo.pilo@eprail.com).

Color versions of one or more of the figures in this paper are available online at http://ieeexplore.ieee.org.

Digital Object Identifier 10.1109/JESTPE.2016.2592938

2168-6777 © 2016 IEEE. Personal use is permitted, but republication/redistribution requires IEEE permission.
See http://www.ieee.org/publications_standards/publications/rights/index.html for more information.

IEEE Proof

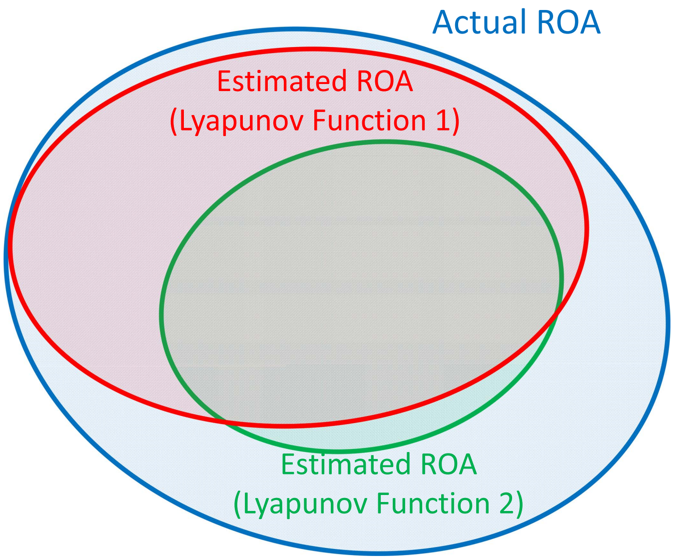

Fig. 1. Domains corresponding to different LFs.

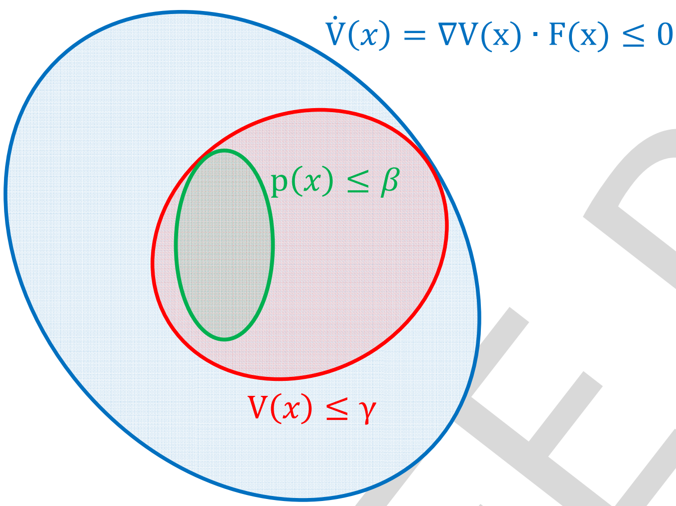

Fig. 2. Set containment formulation of the optimization.

2) *Set B (Red):* Set of the states x for which an arbitrary γ is an upper bound of the LF $V(x)$.
3) *Set C (Blue):* Set of the states x for which $\dot{V}(x)$ is negative. It should be noted that this the only set that directly depends on $F(x)$.
4) Set A $\subseteq$ set B $\subseteq$ set C.

To solve this problem, set A is progressively expanded by increasing β, which in turn expands set B by forcing an increase in γ until the limits of set C are reached. The procedure can be expressed in terms of the following optimization problem:

$$\max\ \beta, \gamma\ \text{ s.t. Set A} \subseteq \text{Set B} \subseteq \text{Set C}. \tag{5}$$

To express the set containment conditions in terms of inequalities, the polynomial S-procedure [11] can be used. Given two sets S_1 and S_2 and two polynomials g_1 and g_2 defined so that

$$\begin{aligned} S_1 &= \{x \in \mathbb{R}^n : g_1(x) \leq 0\} \\ S_2 &= \{x \in \mathbb{R}^n : g_2(x) \leq 0\}. \end{aligned} \tag{6}$$

The polynomial S-procedure establishes that S_1 is included in S_2 if there exists a positive definite polynomial $\lambda(x)$ such that

$$-g_1(x) + \lambda(x) \cdot g_2(x) \text{ is positive definite.} \tag{7}$$

Finally, in order to overcome the difficulty of demonstrating the positive definiteness, the positive definiteness conditions are relaxed into SOS condition, leading to the following formulation of the problem:

$$\max\ \beta, \gamma\ \text{ s.t.}$$
$$V(x) - L_1(x) \text{ is SOS} \tag{8}$$
$$\begin{aligned} &-[\nabla V(x) \cdot F(x) + L_2(x) + s_2(x) \\ &\quad \cdot (\gamma - V(x))] \text{ is SOS} \end{aligned} \tag{9}$$
$$-[(V(x) - \gamma) + s_1(x) \cdot (\beta - p(x))] \text{ is SOS} \tag{10}$$
$$L_1(x) = \epsilon_1 x^T x, \quad L_2(x) = \epsilon_2 x^T x \tag{11}$$

where $L_1(x)$, $L_2(x)$, $s_1(x)$, and $s_2(x)$ are SOS; ϵ_1 and ϵ_2 are arbitrary positive numbers; and $p(x)$ is a fixed SOS polynomial that determines the shape of set A that is progressively enlarged to force set B to grow.

III. Stability-Analysis Algorithm

The optimization problem formulated in (8)–(11) is bilinear in many of the decision variables, namely, the terms $s_2(x) \cdot \gamma$ and $s_2(x) \cdot V(x)$ in (10) and the term $s_1(x) \cdot \beta$ in (11). An SOS problem, however, has to be linear in the decision variables. Hence, an iterative procedure is needed to approximate the bilinear expressions by several consecutive linear approximations [12]. This sequential approximation, referred to as VS iteration, allows one to expand an initial estimation of the ROA. While providing good results in many cases, this procedure has some weaknesses from a practical point of view. First, the selection of the shaping polynomial $p(x)$ can be critical for obtaining a good estimate of the ROA. Unfortunately, the selection of the right $p(x)$ depends on the specific model and is not trivial. Second, the performance of this procedure requires an initial estimation of $V(x)$, which is not always easy to know *a priori*. To overcome the limitations of using a fixed $p(x)$, a double-loop scheme is proposed that sets $p(x) = V(x)$ when the VS iteration has converged to a β and restarts a new VS iteration until $p(x)$ converges. In this paper, two different algorithms have been considered that are outlined in the following and their performances have been evaluated: 1) Algorithm A [captured in (Fig. 3)], which uses a standard VS iteration as outlined in [12], comprises Steps 1–5a and 2) Algorithm B, in which $p(x)$ is updated in each iteration based on $V(x)$, comprises Steps 1–4 and 5b. The steps are described as follows:

1) *Step 1:* To start the VS iteration, a first estimation of the LF is determined using the linear approximation of (3) in the vicinity of the equilibrium point yielding the following:

$$\dot{x} = A \cdot x \tag{12}$$

where A is the Jacobian of $F(x)$. Once A has been determined, if all of its eigenvalues are found to have negative real parts, then there exists a positive-definite

IEEE Proof

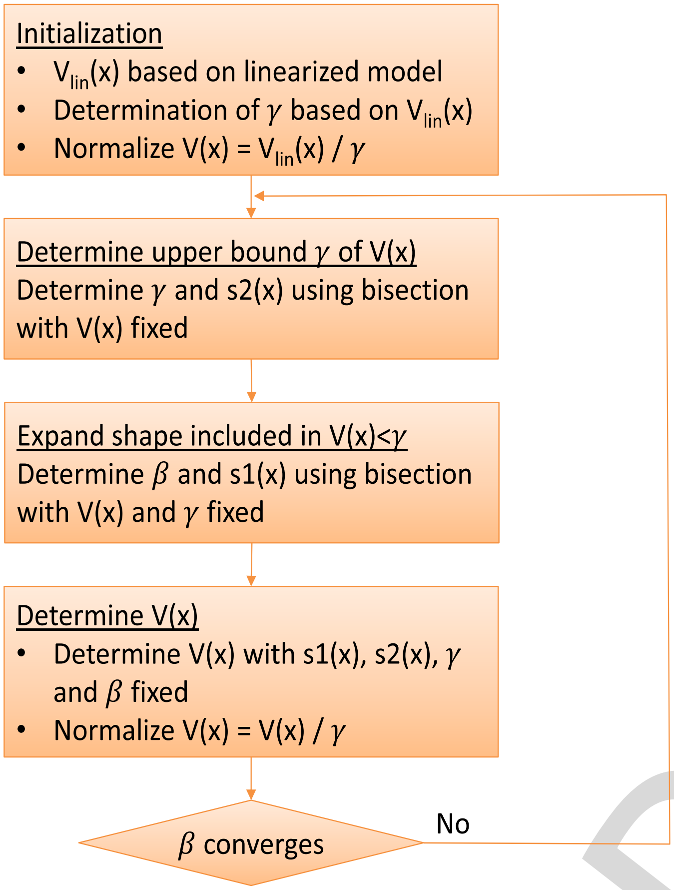

Fig. 3. Set containment formulation of the optimization for Algorithm A. For Algorithm B, only the stop condition is not based on the convergence of β but based on the convergence of $\Delta p(x)$, which is described by (15).

matrix P (where Q must be positive definite) that satisfies the following condition:

$$A^T P + PA + Q = 0. \tag{13}$$

The corresponding LF is determined using

$$V = x^T Px. \tag{14}$$

2) *Step 2:* In this step, $V(x)$ is held fixed while γ and $s_2(x)$ are determined using (9) and (11), using the bisection method to iteratively determine the biggest value of γ.
3) *Step 3:* In this step, $V(x)$ is held fixed while both β and $s_1(x)$ are determined using (10). Because (10) is bilinear in β and $s_1(x)$, bisection is used to obtain $s_1(x)$ while keeping β fixed.
4) *Step 4:* In this step β, γ, $s_1(x)$, and $s_2(x)$ are held fixed while $V(x)$ is determined using (8)–(11) and normalized with respect to γ to avoid numerical problem.
5) *Step 5a:* If the value of β converges, the iteration process is stopped; otherwise, the process flow restarts at Step 2.
6) *Step 5b:* Determine the variation in the shaping function as follows:

$$\Delta p(x) = p(x) - V(x) \tag{15}$$

and subsequently set $p(x) = V(x)$. If the sum of the squares of the coefficients of the polynomial $\Delta p(x)$ attains a value lower than a specified threshold, the iteration process is stopped. Otherwise, the process flow restarts at Step 2.

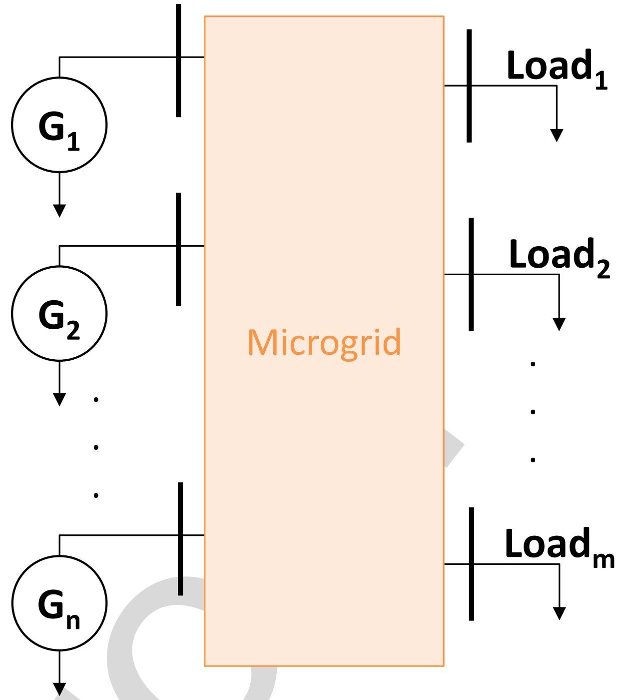

Fig. 4. General topology of the microgrid considered in the study.

It should be noted that in Algorithm B, comparison of the values of β obtained from different iterations does not provide any meaningful information about the convergence because $p(x)$ changes in each of the iterations. Therefore, other criteria such as the N-D volume (referred to as N-volume in this paper) contained inside the ROA have to be used to compare successive estimations of the ROA or the ROAs obtained using different methods.

IV. Dynamic Model of a Multimachine Micropower Network

Fig. 4 shows the structure of the microgrid that has been considered in this paper, which is composed of a set of n synchronous generators (one of whom represents an infinite grid) and m fixed loads, interconnected by electrical lines. Equations (16) and (17) are posed for each generation bus (represented in the left side), while (18) is posed for each load bus. In such a micropower network with n generators, the swing dynamics of the ith generator is given by

$$\dot{\delta}_i = \omega_i \tag{16}$$

$$M_i \dot{\omega}_i = -D_i \omega_i + P_{\mathrm{mec},i} - P_{\mathrm{calc}}(i) \tag{17}$$

where $P_{\mathrm{calc}}(i) = \sum_{j=1}^{N} U_i U_j (G_{\mathrm{ij}} \cos(\delta_{\mathrm{ij}}) + B_{\mathrm{ij}} \sin(\delta_{\mathrm{ij}}))$, $\delta_{\mathrm{ij}} = \delta_i - \delta_j$ is the difference of angles of the voltages at buses i and j, ω_i, D_i, and M_i are, respectively, the angular speed, the damping, and the inertia constant of the generator, $P_{\mathrm{mec},i}$ is the mechanical power fed to the rotor of the generator, U_i is the modulus of the voltage, and G_{ij} and B_{ij} are the real and imaginary parts of the ith and jth elements of the nodal admittance matrix Y_{bus}. If the ith generator is assigned

IEEE Proof

to be the slack generator, (16) is not taken into account because $\delta_i = 0$. If the ith generator is assumed to be infinite, M_i is infinite, and therefore, ω_i is assumed to be constant (i.e., $\dot{\omega}_i = 0$). The power $P_{L,i}$ consumed by the loads at the ith bus is expressed as follows:

$$P_{L,i} = -P_{\text{calc}}(i) \tag{18}$$

where N represents the total number of buses. Equations (16)–(18) are rewritten as a differential-algebraic equation

$$\begin{cases} \dot{X} = F(X, Y) \\ 0 = G(X, Y) \end{cases} \tag{19}$$

where $X = [\delta_1\ \omega_1\ \delta_2\ \omega_2\ \ \ldots]^T$, $Y = [\delta_{N_0}\ \delta_{N_0+1}\ \ \ldots]^T$, and N_0 represents the index of the first load bus, $N_0 + 1$ represents the second load bus, and so on, and

$$F(X, Y) = \begin{bmatrix} \omega_1 \\ -\dfrac{D_1}{M_1}\omega_1 + \dfrac{1}{M_1}(P_{\text{mec},1} - P_{\text{calc}}(1)) \\ \omega_2 \\ -\dfrac{D_2}{M_2}\omega_2 + \dfrac{1}{M_2}(P_{\text{mec},2} - P_{\text{calc}}(2)) \\ \vdots \end{bmatrix}$$

$$G(X, Y) = \begin{bmatrix} -P_{L,N_0} - P_{\text{calc}}(N_0) \\ -P_{L,N_0+1} - P_{\text{calc}}(N_0 + 1) \\ \vdots \end{bmatrix}. \tag{20}$$

Expressing Y in terms of X using the algebraic equation $0 = G(X, Y)$ in (20) and substituting this relationship back in the dynamical model $\dot{X} = F(X, Y)$, one can transform the overall model (20) to solely a state-dependent vector-differential equation that is affine in form. To obtain a dynamical model centered at the origin, the following translation:

$$\omega_i = \Delta\omega_i + \omega_{i,\text{SS}}, \quad \delta_i = \Delta\delta_i + \delta_{i,\text{SS}} \tag{21}$$

is used to obtain the dynamical model in the error coordinates. In (21), $\omega_{i,\text{SS}}$ and $\delta_{i,\text{SS}}$ are the steady-state values for ω_i and δ_i, and $\Delta\omega_i$ and $\Delta\delta_i$ represent the differences between the instantaneous and the equilibrium values of the states. Finally, the resultant model in the error coordinates is expanded using the Taylor series to obtain a dynamical model in polynomial form.

V. Case A: System With No Losses

A. Model Description

The first of the test cases is a fourth-order nonlossy model that has been extensively used as a reference case [13]

$$\begin{cases} \dot{x}_1 = x_2 \\ \dot{x}_2 = -\sin(x_1) - 0.5\sin(x_1 - x_3) - 0.4x_2 \\ \dot{x}_3 = x_4 \\ \dot{x}_4 = -0.5\sin(x_3) - 0.5\sin(x_3 - x_1) - 0.4x_4 + 0.05. \end{cases} \tag{22}$$

The dynamic model (22) has multiple equilibrium points [obtained by equating the right-hand side of (22) to 0]

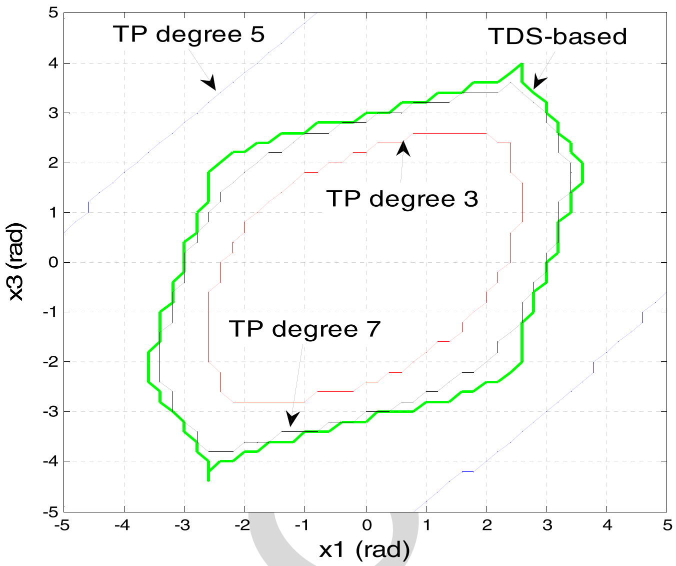

Fig. 5. ROA based on the actual lossless model and the TP model of varying degrees. The estimate of the ROA using TP model of degree 7 yields the best tradeoff between accuracy and computational overhead.

with the nominal equilibrium being ($x_{1,\text{eq}} = 0.02001$, $x_{2,\text{eq}} = 0$, $x_{3,\text{eq}} = 0.06003$, $x_{4,\text{eq}} = 0$). Using this nominal, (22) is translated to the origin yielding the dynamical model

$$\begin{cases} \dot{x}_1 = x_2 \\ \dot{x}_2 = 0.0200\cos(x_1)\cos(x_3) - 0.0200\cos(x_1)\ldots \\ \qquad - 0.9998\sin(x_1) - 0.4x_2\ldots \\ \qquad + 0.4996\cos(x_1)\sin(x_3) - 0.4996\cos(x_3)\sin(x_1)\ldots \\ \qquad + 0.0200\sin(x_1)\sin(x_3) \\ \dot{x}_3 = x_4 \\ \dot{x}_4 = 0.4996\cos(x_3)\sin(x_1) - 0.0299\cos(x_3)\ldots \\ \qquad - 0.4991\sin(x_3) - 0.0200\cos(x_1)\cos(x_3)\ldots \\ \qquad - 0.4996\cos(x_1)\sin(x_3) - 0.5000x_4\ldots \\ \qquad - 0.0200\sin(x_1)\sin(x_3) + 0.0500. \end{cases} \tag{23}$$

Subsequently, using a Taylor series, (23) is converted to Taylor-polynomial (TP) representations of degree 3 and 7 using, respectively, (24) and (25). Accuracies of these TP models are illustrated in Fig. 5 (the best TP estimates are those closer to the TDS-based contour, without trespassing its limits). The degree of the TP approximation is decided keeping an eye on the tradeoff between model accuracy and computational overhead for determining the PLFs and the ROA. For this analysis, the convergence is determined after 5000 time steps of 10 ms each by assessing if the differences between the final and equilibrium values of the state variables are within an N-D sphere (N-sphere) of radius 0.1. To facilitate the analysis of results obtained in this study case, Fig. 6 shows the ROA around the equilibrium point (green area) to which several transients have been superimposed. The initial states are represented with a cross, while the final states are depicted with a circle and a point. The stability conditions ensure that all the trajectories starting inside the ROA will never leave the ROA. Thus, unlike small-signal stability,

IEEE Proof

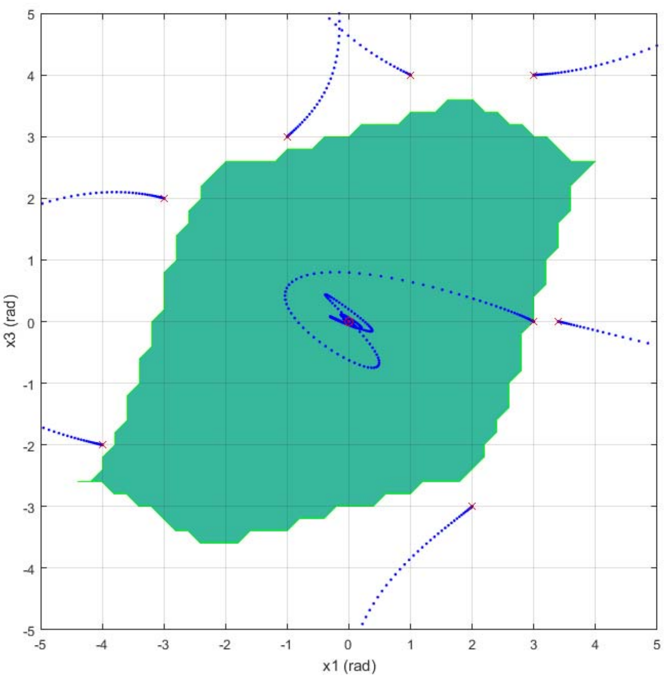

Fig. 6. ROA and time-domain transients in the state-variables space (TDS based, Case A).

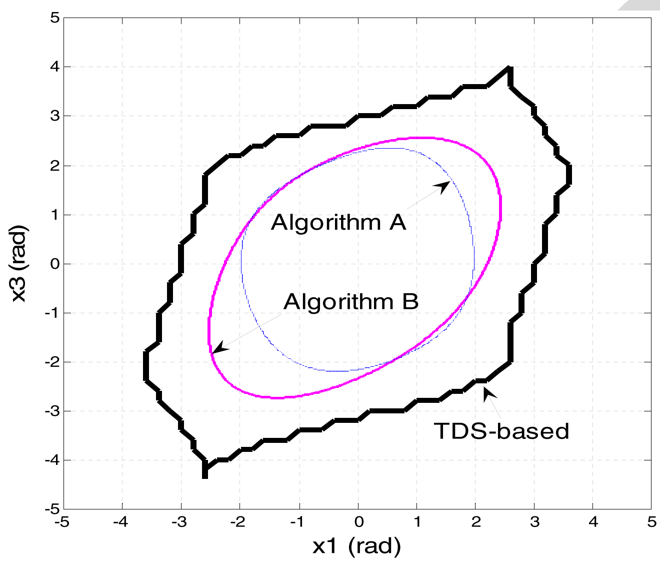

Fig. 7. ROA obtained for Case A with the TP of degree 3.

the PLF-based ROA approach ascertains the large-signal stability of the corresponding equilibrium solution. That is, without doing any TDS, one can ascertain the convergence of an evolving state trajectory if the initial condition lies within the ROA that represents the invariant subspace.

B. Stability Analysis

1) Performance Analysis Using the TP of Degree 3: Fig. 7 shows the ROA obtained using Algorithms A and B using the TP of degree 3 of model (24). The N-volume of the ROAs has been calculated to allow a uniform comparison of the extension of each ROA, independently of the shaping

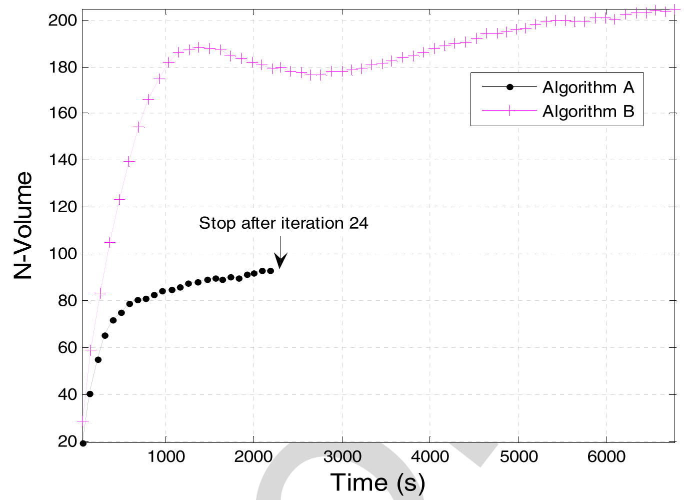

Fig. 8. Progress of ROA estimation with the time for Case A with the TP of degree 3.

function used in each case

$$\begin{cases} \dot{x}_1 = x_2 \\ \dot{x}_2 = 0.2499x_1^3 - 0.2498x_1^2x_3 + 0.2498x_1x_3^2 + \dots \\ \quad - 0.083267x_3^3 + 0.019995x_1x_3 - 0.0099973x_3^2 \dots \\ \quad - 1.4994x_1 - 0.4x_2 + 0.4996x_3 \\ \dot{x}_3 = x_4 \\ \dot{x}_4 = -0.083267x_1^3 + 0.2498x_1^2x_3 - 0.2498x_1x_3^2 \\ \quad + 0.16645x_3^3 + 0.0099973x_1^2 - 0.019995x_1x_3 \dots \\ \quad + 0.024988x_3^2 + 0.4996x_1 - 0.9987x_3 - 0.5x_4 \end{cases} \tag{24}$$

$$\begin{cases} \dot{x}_1 = x_2 \\ \dot{x}_2 = 0.0020817x_1^5x_3^2 - 0.0034694x_1^4x_3^3 \dots \\ \quad + 0.0034694x_1^3x_3^4 - 0.0020817x_1^2x_3^5 \\ \quad - 0.012495x_1^5 \dots + 0.020817x_1^4x_3 - 0.041633x_1^3x_3^2 \\ \quad + 0.041633x_1^2x_3^3 \dots - 0.020817x_1x_3^4 + 0.0041633x_3^5 \\ \quad - 0.0033324x_1^3x_3 \dots + 0.0049987x_1^2x_3^2 \\ \quad - 0.0033324x_1x_3^3 + 0.2499x_1^3 \dots \\ \quad - 0.2498x_1^2x_3 + 0.2498x_1x_3^2 - 0.083267x_3^3 \dots \\ \quad + 0.019995x_1x_3 - 0.0099973x_3^2 - 1.4994x_1 \dots \\ \quad - 0.4x_2 + 0.4996x_3 \\ \dot{x}_3 = x_4 \\ \dot{x}_4 = -0.0020817x_1^5x_3^2 + 0.0034694x_1^4x_3^3 \dots \\ \quad - 0.0034694x_1^3x_3^4 + 0.0020817x_1^2x_3^5 \\ \quad + 0.0041633x_1^5 \dots - 0.020817x_1^4x_3 + 0.041633x_1^3x_3^2 \\ \quad - 0.041633x_1^2x_3^3 \dots + 0.020817x_1x_3^4 + 0.0083225x_3^5 \\ \quad + 0.0033324x_1^3x_3 \dots - 0.0049987x_1^2x_3^2 \\ \quad + 0.0033324x_1x_3^3 - 0.0020824x_3^4 \dots \\ \quad - 0.083267x_1^3 + 0.2498x_1^2x_3 - 0.2498x_1x_3^2 \dots \\ \quad + 0.16645x_3^3 + 0.0099973x_1^2 - 0.019995x_1x_3 \dots \\ \quad + 0.024988x_3^2 - 0.4996x_1 - 0.5x_2 + 0.9987x_3. \end{cases} \tag{25}$$

The Monte Carlo-based function p-volume approach [14] has been used for determining the N-volumes. Fig. 8 compares

TABLE I

$V(x)$ FOR CASE A OBTAINED WITH THE TP OF DEGREE 3 AND ALGORITHM A

Coefficients	Degree				Coefficients	Degree				Coefficients	Degree				Coefficients	Degree			
	X1	X2	X3	X4		X1	X2	X3	X4		X1	X2	X3	X4		X1	X2	X3	X4
0.040735082	4	0	0	0	-0.006064559	1	0	2	1	0.051053757	0	0	0	4	-0.002091286	0	0	3	0
0.021256957	3	1	0	0	-0.00203639	1	0	1	2	0.000531507	3	0	0	0	0.005433244	0	0	2	1
0.038096939	3	0	1	0	0.029249162	1	0	0	3	-0.010999359	2	1	0	0	0.004023011	0	0	1	2
-0.007345416	3	0	0	1	0.024442941	0	4	0	0	-0.001439241	2	0	1	0	-0.000727138	0	0	0	3
0.051291872	2	2	0	0	-0.043553995	0	3	1	0	0.010330181	2	0	0	1	0.093052692	2	0	0	0
-0.012767702	2	1	1	0	0.030431778	0	3	0	1	-0.012637191	1	2	0	0	-0.090809789	1	1	0	0
0.043364697	2	1	0	1	0.066993481	0	2	2	0	0.002837382	1	1	1	0	0.015305361	1	0	1	0
0.105240173	2	0	2	0	0.012700488	0	2	1	1	0.007474406	1	1	0	1	-0.012990328	1	0	0	1
0.029198532	2	0	1	1	0.100795961	0	2	0	2	0.001186083	1	0	2	0	0.084143381	0	2	0	0
0.098596463	2	0	0	2	0.008793697	0	1	3	0	-0.002915266	1	0	1	1	0.01421332	0	1	1	0
-0.013880525	1	3	0	0	0.037927366	0	1	2	1	-0.008659004	1	0	0	2	0.045274049	0	1	0	1
0.060439883	1	2	1	0	-0.00572891	0	1	1	2	-0.006410801	0	3	0	0	0.050885332	0	0	2	0
0.012639839	1	2	0	1	0.003365759	0	1	0	3	-0.016324434	0	2	1	0	-0.007716157	0	0	1	1
0.018079848	1	1	2	0	0.045370358	0	0	4	0	0.003177474	0	2	0	1	0.063755529	0	0	0	2
0.002940689	1	1	1	1	0.031689761	0	0	3	1	-0.011730248	0	1	2	0					
-0.024567091	1	1	0	2	0.067467103	0	0	2	2	-0.005649717	0	1	1	1					
0.01557886	1	0	3	0	0.022770203	0	0	1	3	-0.004380363	0	1	0	2					

TABLE II

$V(x)$ FOR CASE A OBTAINED WITH THE TP OF DEGREE 3 AND ALGORITHM B

Coefficients	Degree				Coefficients	Degree				Coefficients	Degree				Coefficients	Degree			
	X1	X2	X3	X4		X1	X2	X3	X4		X1	X2	X3	X4		X1	X2	X3	X4
0.009250389	4	0	0	0	0.012842272	1	0	2	1	0.005556495	0	0	0	4	0.001885302	0	0	3	0
0.007702928	3	1	0	0	-0.005785044	1	0	1	2	0.002114628	3	0	0	0	0.013920166	0	0	2	1
0.015229751	3	0	1	0	0.007043757	1	0	0	3	-0.002685473	2	1	0	0	0.034579883	0	0	1	2
-0.004557754	3	0	0	1	0.00708155	0	4	0	0	0.000222118	2	0	1	0	-0.004149076	0	0	0	3
-0.002084968	2	2	0	0	-0.004364719	0	3	1	0	0.012925707	2	0	0	1	0.153636156	2	0	0	0
0.020746695	2	1	1	0	0.012377532	0	3	0	1	0.011349252	1	2	0	0	-0.224865341	1	1	0	0
-0.004982327	2	1	0	1	0.020601264	0	2	2	0	0.015321788	1	1	1	0	0.060129875	1	0	1	0
0.043019094	2	0	2	0	0.015375107	0	2	1	1	0.013540199	1	1	0	1	0.00043507	1	0	0	1
0.000719135	2	0	1	1	0.014745112	0	2	0	2	0.005718536	1	0	2	0	0.143805684	0	2	0	0
0.02008912	2	0	0	2	0.018721951	0	1	3	0	0.002912879	1	0	1	1	-0.102635351	0	1	1	0
0.004843946	1	3	0	0	-9.91E-05	0	1	2	1	-0.006416794	1	0	0	2	0.122289495	0	1	0	1
0.014608679	1	2	1	0	0.029342739	0	1	1	2	0.00056016	0	3	0	0	0.078608858	0	0	2	0
0.02486459	1	2	0	1	-0.003386151	0	1	0	3	-0.010808744	0	2	1	0	-0.112724937	0	0	1	1
0.006053929	1	1	2	0	0.013908916	0	0	4	0	0.014262814	0	2	0	1	0.157712782	0	0	0	2
-0.021833346	1	1	1	1	0.001027484	0	0	3	1	0.004302414	0	1	2	0					
-0.001008285	1	1	0	2	0.019030519	0	0	2	2	0.022433579	0	1	1	1					
0.003474922	1	0	3	0	-0.001219043	0	0	1	3	0.010858378	0	1	0	2					

the temporal evolution of the N-volume of the ROA estimated with Algorithms A and B. All the tested algorithms show a big improvement of the ROA estimation in the first iterations followed by a slowing down phase. Table I shows the polynomials obtained using Algorithm A ($\beta = 3.2860$ and $\gamma = 1.0002$ that following Steps 2 and 3 are obtained using the bisection method over a prespecified range of 0.01–100 for both the parameters). It shows how the PLF is dependent on the state variables and the coefficients corresponding to these state variables with varying degrees that are also indicated in Table I. Table II shows the polynomials obtained using Algorithm B ($\beta = 0.6645$ and $\gamma = 1.0002$). The executions

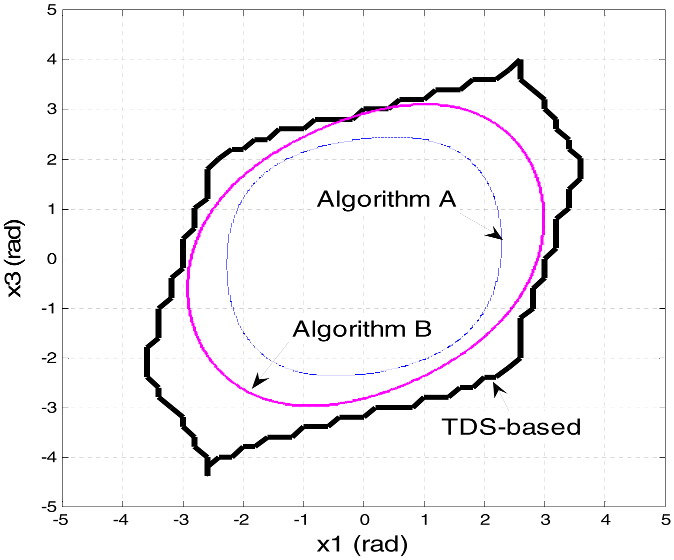

Fig. 9. ROA obtained for Case A with the TP of degree 7.

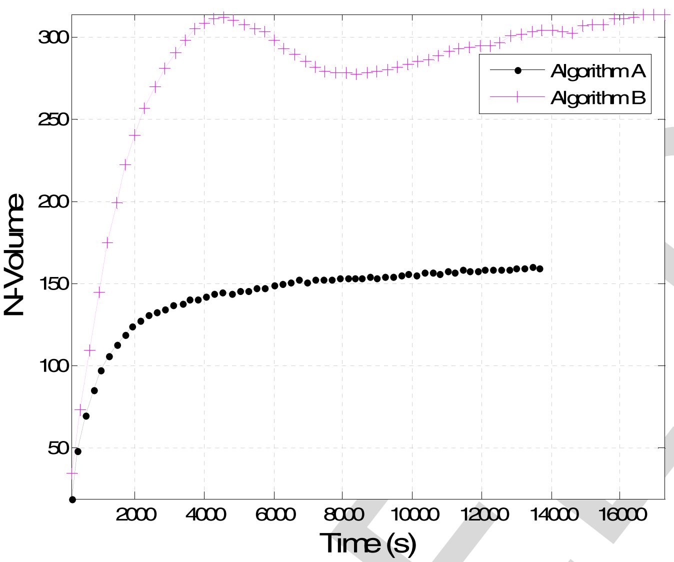

Fig. 10. Progress of ROA estimation with the time for Case A with the TP of degree 7.

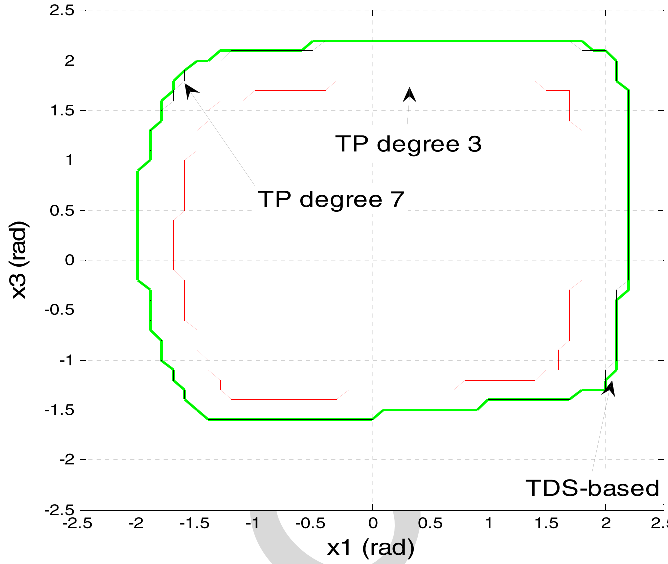

Fig. 11. ROA based on the actual lossy model and the TP model of degrees 3 and 7.

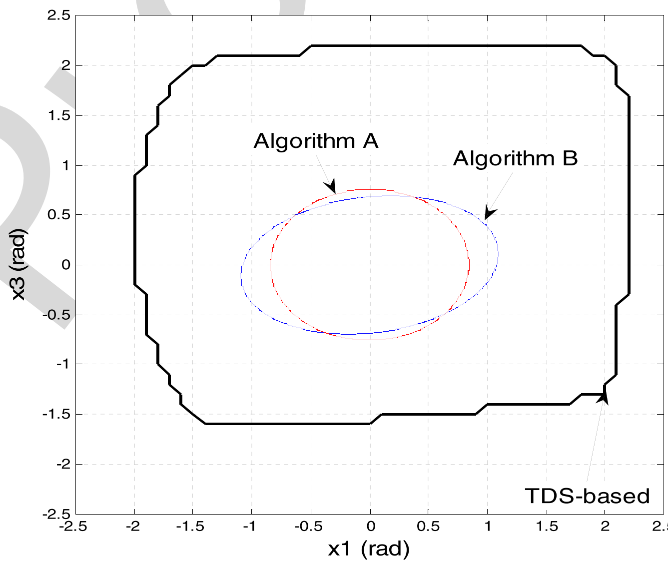

Fig. 12. ROA obtained for Case B with the TP of degree 3.

of Algorithm A stopped after iteration 24, before reaching the maximum number of iterations (which was set to 60), when the variation of β was lower than 0.05% of its value. The N-volume always increased until the increase is sufficiently small. On the other hand, Algorithm B achieves a better estimation of the ROA because of its ability to adapt $p(x)$, but it is not guaranteed to monotonically converge to the largest ROA and can incur some small oscillations as observed in Fig. 8.

2) Performance Analysis Using the TP of Degree 7: Fig. 9 shows the ROA obtained using Algorithms A and B using the TP of degree 7 of model (25). Table III shows the polynomials obtained using Algorithm A ($\beta = 4.4083$ and $\gamma = 1.0002$). Table IV shows the polynomials obtained using Algorithm B ($\beta = 0.7477$ and $\gamma = 1.0002$). Fig. 10 compares the temporal evolution of the N-volume of the ROA estimated using Algorithms A and B. All executions of Algorithms A and B stop when the maximum number of iterations (which is set at 60) is reached. Each iteration takes a different amount of time depending on the degree of the polynomials and the algorithm used. For each iteration, N-volume of the ROA estimate increases for Algorithm A, whereas Algorithm B yields a better estimate of the ROA relatively faster, but may incur small oscillations.

VI. Case B: System With Losses

A. Model Description

The second test case is a fourth-order model (26) with losses, which has been used in the literature as a reference case [13]. In (26), $x_{\text{ij}} = x_i - x_j$. The nominal equilibrium

TABLE III
$V(x)$ FOR CASE A OBTAINED WITH THE TP OF DEGREE 7 AND ALGORITHM A

Coefficients	Degree			
	X1	X2	X3	X4
0.024237165	4	0	0	0
0.003502696	3	1	0	0
0.028464694	3	0	1	0
-0.008340299	3	0	0	1
0.014884319	2	2	0	0
0.020807307	2	1	1	0
0.007884523	2	1	0	1
0.050903748	2	0	2	0
0.019921558	2	0	1	1
0.033891749	2	0	0	2
-0.002374239	1	3	0	0
0.025465494	1	2	1	0
0.039232708	1	2	0	1
-0.019328653	1	1	2	0
0.011978601	1	1	1	1
-0.022900003	1	1	0	2
0.008126687	1	0	3	0

Coefficients	Degree			
	X1	X2	X3	X4
-0.005073733	1	0	2	1
-0.009319127	1	0	1	2
0.007185712	1	0	0	3
0.01113434	0	4	0	0
-0.018960184	0	3	1	0
0.00010111	0	3	0	1
0.031340216	0	2	2	0
0.017932473	0	2	1	1
0.026861435	0	2	0	2
0.006951314	0	1	3	0
0.017475377	0	1	2	1
-0.00286558	0	1	1	2
-0.019891088	0	1	0	3
0.020075952	0	0	4	0
-0.001734241	0	0	3	1
0.033468229	0	0	2	2
-0.002684603	0	0	1	3

Coefficients	Degree			
	X1	X2	X3	X4
0.009182625	0	0	0	4
7.43E-05	3	0	0	0
-0.007368648	2	1	0	0
-0.001020734	2	0	1	0
0.00157876	2	0	0	1
0.002467297	1	2	0	0
0.0100079	1	1	1	0
0.00351494	1	1	0	1
0.002099053	1	0	2	0
-0.001081407	1	0	1	1
-0.011507457	1	0	0	2
-0.003226796	0	3	0	0
0.003191054	0	2	1	0
0.011283193	0	2	0	1
-0.003680113	0	1	2	0
0.002131538	0	1	1	1
-0.002204134	0	1	0	2

Coefficients	Degree			
	X1	X2	X3	X4
-0.00262985	0	0	3	0
0.003779334	0	0	2	1
0.003533487	0	0	1	2
-0.004060268	0	0	0	3
0.068408428	2	0	0	0
-0.055345734	1	1	0	0
0.02769111	1	0	1	0
-0.002969704	1	0	0	1
0.114772267	0	2	0	0
-0.0042432	0	1	1	0
0.110003933	0	1	0	1
0.040018155	0	0	2	0
0.021222384	0	0	1	1
0.163920445	0	0	0	2

TABLE IV
$V(x)$ FOR CASE A OBTAINED WITH THE TP OF DEGREE 7 AND ALGORITHM B

Coefficients	Degree			
	X1	X2	X3	X4
0.004707302	4	0	0	0
0.003439435	3	1	0	0
0.012016978	3	0	1	0
-0.004043872	3	0	0	1
0.003425216	2	2	0	0
0.01105376	2	1	1	0
0.002616668	2	1	0	1
0.030317731	2	0	2	0
-0.002811025	2	0	1	1
0.00829066	2	0	0	2
0.001347748	1	3	0	0
0.00788031	1	2	1	0
0.014399093	1	2	0	1
0.004651303	1	1	2	0
-0.003275689	1	1	1	1
-0.003011419	1	1	0	2
0.00840209	1	0	3	0

Coefficients	Degree			
	X1	X2	X3	X4
0.003917303	1	0	2	1
-0.001512618	1	0	1	2
-0.000137389	1	0	0	3
0.001512299	0	4	0	0
-0.003078052	0	3	1	0
0.002176528	0	3	0	1
0.014527924	0	2	2	0
0.00591549	0	2	1	1
0.006560786	0	2	0	2
0.011756457	0	1	3	0
-0.000230325	0	1	2	1
0.017087984	0	1	1	2
-0.008504258	0	1	0	3
0.011727397	0	0	4	0
0.005697032	0	0	3	1
0.01234465	0	0	2	2
-0.005436832	0	0	1	3

Coefficients	Degree			
	X1	X2	X3	X4
0.003626706	0	0	0	4
-0.000398442	3	0	0	0
-0.003159629	2	1	0	0
0.000544575	2	0	1	0
0.002405031	2	0	0	1
-0.00010191	1	2	0	0
0.006318496	1	1	1	0
0.011274232	1	1	0	1
0.002043134	1	0	2	0
0.004287611	1	0	1	1
-0.009913395	1	0	0	2
-0.001523572	0	3	0	0
-0.006402178	0	2	1	0
0.009615392	0	2	0	1
-0.001238954	0	1	2	0
0.008686647	0	1	1	1
-0.001594697	0	1	0	2

Coefficients	Degree			
	X1	X2	X3	X4
0.003752754	0	0	3	0
0.014989886	0	0	2	1
0.019448094	0	0	1	2
-0.001506097	0	0	0	3
0.082138061	2	0	0	0
-0.098457538	1	1	0	0
0.03313441	1	0	1	0
0.026543699	1	0	0	1
0.108929361	0	2	0	0
-0.060812283	0	1	1	0
0.098805079	0	1	0	1
0.045162891	0	0	2	0
-0.02654665	0	0	1	1
0.161543478	0	0	0	2

of (26) is ($x_{1,\mathrm{eq}} = 0.4680$, $x_{2,\mathrm{eq}} = 0$, $x_{3,\mathrm{eq}} = 0.04630$, $x_{4,\mathrm{eq}} = 0$). Using this nominal equilibrium and following Section IV, (26) is transformed to a TP representation of degrees 3 and 7, respectively, as captured in (27) and (28) (see the next page). Accuracies of these TP models are illustrated in Fig. 11, where convergence is determined after 5000 time steps of 10 ms each by assessing if the differences between the final and equilibrium values of the state variables

TABLE V
$V(x)$ FOR CASE B OBTAINED WITH THE TP OF DEGREE 3 AND ALGORITHM A

Coefficients	Degree				Coefficients	Degree				Coefficients	Degree				Coefficients	Degree			
	X1	X2	X3	X4		X1	X2	X3	X4		X1	X2	X3	X4		X1	X2	X3	X4
1.4009314	2	0	0	0	0.0679309	1	0	0	1	0.0253620	0	1	0	1	0.0192381	0	0	0	2
-0.0219146	1	1	0	0	1.7336369	0	2	0	0	0.0231047	0	0	2	0					
0.0624902	1	0	1	0	-0.0699996	0	1	1	0	0.0089387	0	0	1	1					

TABLE VI
$V(x)$ FOR CASE B OBTAINED WITH THE TP OF DEGREE 3 AND ALGORITHM B

Coefficients	Degree				Coefficients	Degree				Coefficients	Degree				Coefficients	Degree			
	X1	X2	X3	X4		X1	X2	X3	X4		X1	X2	X3	X4		X1	X2	X3	X4
0.8556518	2	0	0	0	0.0058081	1	0	0	1	0.0410336	0	1	0	1	0.0221799	0	0	0	2
-0.4316670	1	1	0	0	2.1150377	0	2	0	0	0.0136756	0	0	2	0					
0.0384129	1	0	1	0	-0.0045906	0	1	1	0	-0.0000091	0	0	1	1					

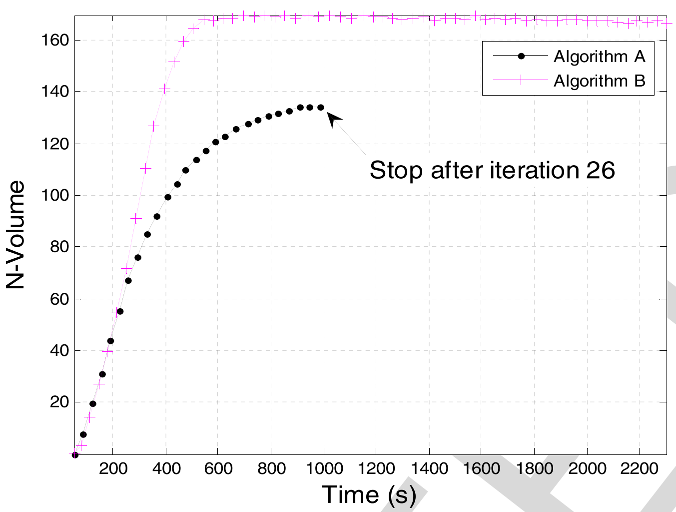

Fig. 13. Progress of ROA estimation with the time for Case B with the TP of degree 3.

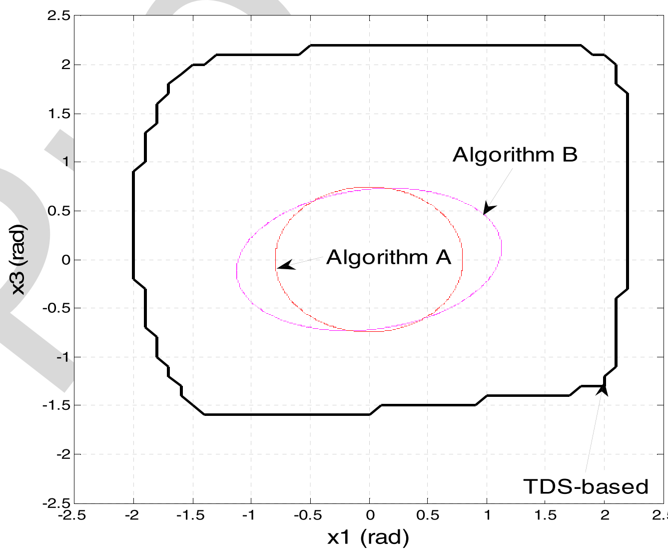

Fig. 14. ROA obtained for Case B with the TP of degree 7.

are within an N-sphere of radius 0.1

$$\begin{cases} \dot{x}_1 = x_2 \\ \dot{x}_2 = 33.5849 - 1.8868\cos(x_{13}) - 5.2830\cos(x_1) \\ -16.9811\sin(x_{13}) - 59.6226\sin(x_1) - 1.8868x_2 \\ \dot{x}_3 = x_4 \\ \dot{x}_4 = 48.4810 + 11.3924\sin(x_{13}) - 1.2658\cos(x_{13}) \\ -3.2278\cos(x_3) - 99.3671\sin(x_3) - 1.2658x_4 \end{cases} \tag{26}$$

$$\begin{cases} \dot{x}_1 = x_2 \\ \dot{x}_2 = 11.3x_1^3 - 8.4857x_1^2x_3 + 8.4857x_1x_3^2 \dots \\ -2.8286x_3^3 + 16.7913x_1^2 - 1.9717x_1x_3 \dots \\ +0.98584x_3^2 - 67.7998x_1 + 16.9715x_3 - 1.8868x_2 \\ \dot{x}_3 = x_4 \\ \dot{x}_4 = -1.8998x_1^3 + 5.6993x_1^2x_3 - 5.6993x_1x_3^2 \dots \\ +16.4771x_3^3 + 0.60441x_1^2 - 1.2088x_1x_3 \dots \\ +24.2388x_3^2 + 11.3986x_1 - 98.8623x_3 - 1.2658x_4. \end{cases} \tag{27}$$

B. Stability Analysis

1) Performance Analysis Using the TP of Degree 3: Fig. 12 shows the ROA obtained using Algorithms A and B using the TP of degree 3 of model (27). Fig. 13 compares the temporal evolution of the N-volume of the ROA estimated using Algorithms A and B. Algorithm B yields a better estimate of the ROA relatively faster (with minimal oscillations) compared with Algorithm A. Table V shows the polynomials obtained using Algorithm A ($\beta = 0.5760$ and $\gamma = 1.0002$). Table VI shows the polynomials obtained using Algorithm B ($\beta = 0.9834$ and $\gamma = 0.9995$). As indicated in the description of the algorithms (see Steps 2 and 3), γ and β are obtained using the bisection method over a prespecified range (in this case, the range [0.01, 100] for both parameters).

2) Performance Analysis Using the TP of Degree 7: Fig. 14 shows the ROA obtained using Algorithms A and B using the TP of degree 7 of model (28). Fig. 15 compares the temporal evolution of the N-volume of the ROA estimated

IEEE Proof

TABLE VII

$V(x)$ FOR CASE B OBTAINED WITH THE TP OF DEGREE 7 AND ALGORITHM A

Coefficients	Degree				Coefficients	Degree				Coefficients	Degree				Coefficients	Degree			
	X1	X2	X3	X4		X1	X2	X3	X4		X1	X2	X3	X4		X1	X2	X3	X4
1.5638250	2	0	0	0	0.0701764	1	0	0	1	0.0227691	0	1	0	1	0.0198351	0	0	0	2
-0.0082497	1	1	0	0	1.8004734	0	2	0	0	0.0257472	0	0	2	0					
0.0562647	1	0	1	0	-0.0773480	0	1	1	0	0.0093440	0	0	1	1					

TABLE VIII

$V(x)$ FOR CASE B OBTAINED WITH THE TP OF DEGREE 7 AND ALGORITHM B

Coefficients	Degree				Coefficients	Degree				Coefficients	Degree				Coefficients	Degree			
	X1	X2	X3	X4		X1	X2	X3	X4		X1	X2	X3	X4		X1	X2	X3	X4
0.8110194	2	0	0	0	0.0122084	1	0	0	1	0.0363584	0	1	0	1	0.0202649	0	0	0	2
-0.4079839	1	1	0	0	1.9250915	0	2	0	0	0.0130368	0	0	2	0					
0.0354819	1	0	1	0	-0.0124661	0	1	1	0	0.0000345	0	0	1	1					

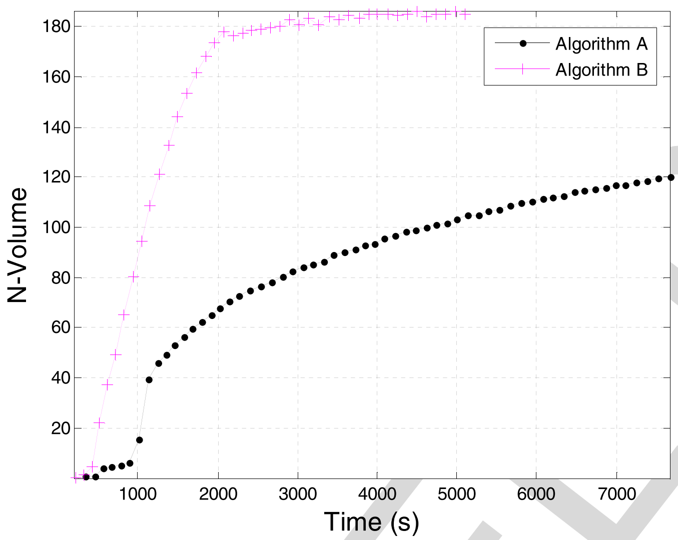

Fig. 15. Progress of ROA estimation with the time for Case B with the TP of degree 7.

with Algorithms A and B. Convergence of Algorithm B is faster, with no oscillations. Table VII shows the polynomials obtained using Algorithm A ($\beta = 0.5542$ and $\gamma = 1.0010$). Table VIII shows the polynomials obtained using Algorithm B ($\beta = 0.9850$ and $\gamma = 1.0010$).

VII. CONCLUSION

An investigation into the effectiveness of polynomial-Lyapunov-function-based methodology for stability analysis of a micropower network is outlined. While the condition of LF-based stability analysis remains the same, what is different is how the LF is determined autonomously using a semidefinite optimization-based methodology along with determining the ROA of the equilibrium solution without using computationally intensive time-domain solution. Furthermore, two algorithms are outlined and the mechanism and their efficacies and convergence analyses are illustrated for a lossless and a lossy dynamical system model

$$\begin{cases} \dot{x}_1 = x_2 \\ \dot{x}_2 = 0.013452x_1^7 - 0.023571x_1^6x_3 + 0.070714x_1^5x_3^2 \ldots \\ -0.11786x_1^4x_3^3 + 0.11786x_1^3x_3^4 - 0.070714x_1^2x_3^5 \ldots \\ +0.023571x_1x_3^6 - 0.0033674x_3^7 + 0.046642x_1^6 \ldots \\ -0.016431x_1^5x_3 + 0.041077x_1^4x_3^2 - 0.054769x_1^3x_3^3 \ldots \\ +0.041077x_1^2x_3^4 - 0.016431x_1x_3^5 + 0.0027384x_3^6 \ldots \\ -0.565x_1^5 + 0.70714x_1^4x_3 - 1.4143x_1^3x_3^2 \ldots \\ +1.4143x_1^2x_3^3 - 0.70714x_1x_3^4 + 0.14143x_3^5 \ldots \\ -1.3993x_1^4 + 0.32861x_1^3x_3 - 0.49292x_1^2x_3^2 \ldots \\ +0.32861x_1x_3^3 - 0.082153x_3^4 + 11.3x_1^3 \ldots \\ -8.4857x_1^2x_3 + 8.4857x_1x_3^2 - 2.8286x_3^3 \ldots \\ +16.7913x_1^2 - 1.9717x_1x_3 + 0.98584x_3^2 \ldots \\ -67.7998x_1 + 16.9715x_3 - 1.8868x_2 \\ \dot{x}_3 = x_4 \\ \dot{x}_4 = -0.0022616x_1^7 + 0.015831x_1^6x_3 - 0.047494x_1^5x_3^2 \ldots \\ +0.079157x_1^4x_3^3 - 0.079157x_1^3x_3^4 + 0.047494xx_1^2x_3^5 \ldots \\ -0.015831x_1x_3^6 + 0.019616x_3^7 + 0.0016789x_1^6 \ldots \\ -0.010074x_1^5x_3 + 0.025184x_1^4x_3^2 - 0.033578x_1^3x_3^3 \ldots \\ +0.025184x_1^2x_3^4 - 0.010074x_1x_3^5 + 0.06733x_3^6 \ldots \\ +0.094988x_1^5 - 0.47494x_1^4x_3 + 0.94988x_1^3x_3^2 \ldots \\ -0.94988x_1^2x_3^3 + 0.47494x_1x_3^4 - 0.82385x_3^5 \ldots \\ -0.050368x_1^4 + 0.20147x_1^3x_3 - 0.30221x_1^2x_3^2 \ldots \\ +0.20147x_1x_3^3 - 2.0199x_3^4 - 1.8998x_1^3 \ldots \\ +5.6993x_1^2x_3 - 5.6993x_1x_3^2 + 16.4771x_3^3 \ldots \\ +0.60441x_1^2 - 1.2088x_1x_3 + 24.2388x_3^2 \ldots \\ +11.3986x_1 - 98.8623x_3 - 1.2658x_4. \end{cases} \tag{28}$$

IEEE Proof

ACKNOWLEDGMENT

The authors acknowledge the use of following softwares: SOSTOOLS 2.05, SeDuMi 1.3, and Multipoly 2.00. However, any opinions, findings, conclusions, or recommendations expressed herein are those of the authors and do not necessarily reflect the views of the DOE or the NSF.

REFERENCES

[1] C. Wang, Y. Li, K. Peng, B. Hong, Z. Wu, and C. Sun, "Coordinated optimal design of inverter controllers in a micro-grid with multiple distributed generation units," *IEEE Trans. Power Syst.*, vol. 28, no. 3, pp. 2679–2687, Aug. 2013, doi: 10.1109/TPWRS.2013.2245922.

[2] F. Katiraei, M. R. Iravani, and P. W. Lehn, "Small-signal dynamic model of a micro-grid including conventional and electronically interfaced distributed resources," *IET Generat., Transmiss. Distrib.*, vol. 1, no. 3, pp. 369–378, May 2007, doi: 10.1049/iet-gtd:20045207.

[3] A. Arapostathis, S. Sastry, and P. Varaiya, "Global analysis of swing dynamics," *IEEE Trans. Circuits Syst.*, vol. 29, no. 10, pp. 673–679, Oct. 1982.

[4] H. K. Khalil, *Nonlinear Systems*. Englewood Cliffs, NJ, USA: Prentice-Hall, 2002.

[5] S.K. Mazumder, "Nonlinear analysis and control of standalone, parallel DC-DC, and parallel multi-phase PWM converters," Ph.D. dissertation, Dept. Elect. Comput. Eng., Virginia Tech, Blacksburg, VA, USA, 2001.

[6] S. K. Mazumder and E. Pilo de la Fuente, "Dynamic stability analysis of power network," in *Proc. IEEE Energy Convers. Conf. Expo.*, Sep. 2015, pp. 5808–5815.

[7] M. Vidyasagar, *Nonlinear Systems Analysis*. Philadelphia, PA, USA: SIAM, 2002.

[8] S. K. Mazumder and K. Acharya, "Multiple Lyapunov function based reaching condition for orbital existence of switching power converters," *IEEE Trans. Power Electron.*, vol. 23, no. 3, pp. 1449–1471, May 2008.

[9] S. K. Mazumder and E. P. de la Fuente, "Transient stability analysis of power system using polynomial Lyapunov function based approach," in *Proc. IEEE PES GM*, Jul. 2014, pp. 1–5, doi: 10.1109/PESGM.2014.6939524.2014.

[10] J. B. Lasserre, "Global optimization with polynomials and the problem of moments," *SIAM J. Optim.*, vol. 11, no. 3, pp. 796–817, 2001.

[11] P. A. Parillo, "Structured semidefinite programs and semialgebraic geometry methods in robustness and optimization," Ph.D. dissertation, California Inst. Technol., Pasadena, CA, USA, 2000.

[12] A. Chakraborty, P. Seiler, and G. J. Balas, "Susceptibility of F/A-18 flight controllers to the falling-leaf mode: Nonlinear analysis," *J. Guid., Control, Dyn.*, vol. 34, no. 1, pp. 73–85, 2011.

[13] H.-D. Chang, C.-C. Chu, and G. Cauley, "Direct stability analysis of electric power systems using energy functions: Theory, applications, and perspective," *Proc. IEEE*, vol. 83, no. 11, pp. 1497–1529, Nov. 1995.

[14] G. J. Balas, A. Packard, P. Seiler, and U. Topcu. (2009). *Robustness Analysis of Nonlinear Systems*. [Online]. Available: http://www.aem.umn.edu/~AerospaceControl/

Sudip K. Mazumder (F'16–SM'03) received the M.S. degree in electrical power engineering from the Rensselaer Polytechnic Institute, Troy, NY, USA, in 1993, and the Ph.D. degree in electrical and computer engineering from the Virginia Polytechnic Institute and State University, Blacksburg, VA, USA, in 2001.

He is currently a Professor with the Department of Electrical and Computer Engineering, University of Illinois at Chicago (UIC), Chicago, IL, USA, and the Director of the Laboratory for Energy and Switching-Electronics Systems. He has over 24 years of professional experience and has held R&D and design positions in leading industrial organizations and has served as a Technical Consultant for several industries. He also serves as the President of NextWatt LLC, Hoffman Estates, IL, USA, a small business organization that he setup in 2008. He has presented 75 invited/plenary/keynote presentations and holds eight issued patents with several pending. He has authored over 200 refereed papers in prestigious journals and conferences and has authored one book and nine book chapters.

Dr. Mazumder has been awarded about 40 sponsored projects by NSF, DOE, ONR, CEC, EPA, AFRL, NASA, ARPA-E, NAVSEA, and multiple leading industries in above-referenced areas, since joining UIC. In 2013, he was a recipient of the University of Illinois' Highest Award–University Scholar Award. In 2014, he was a recipient of the Inventor of the Year Award at UIC. He was a recipient of the NSF Career Award in 2003, the ONR Young Investigator Award in 2005, and the PELS Transaction Prize Paper Award in 2002. Since 2015, he has served as the Chair for the IEEE Power Electronics Society (PELS) Technical Committee on Sustainable Energy Systems. Since 2016, he has served as a Distinguished Lecturer for the IEEE PELS.

Eduardo Pilo de la Fuente (SM'15) received the Ph.D. degree from the Engineering School, Universidad Pontificia Comillas, Madrid, Spain, in 2003.

He served as a Researcher with the Institute for Research in Technology (Comillas), the Railways Group (ASF), and the Power System Modeling Group, from 2003 to 2010. Since 2003, he has been a Lecturer of several degrees, and master's and doctorate courses related to power systems and railways. From 2010 to 2012, he was with the Electrical Industry as a Consultant of Multitest09, Madrid. In 2012, he founded his own company (EPRail Research and Consulting, SL), and since then, he has been involved in providing research and consultancy services in the field of power systems and railways. From 2013 to 2014, he was a Visiting Professor and Research Scientist with the University of Illinois at Chicago, Chicago, IL, USA. His expertise comprises the modeling, simulation, and analysis of railway power systems, including their interrelations with transmission and distribution grids. He has conducted research and consultancy for major companies/bodies in the railway and electrical sectors, such as ADIF–the Spanish Railways Infrastructure Manager, Renfe, SEMI, Cobra, Gas Natural Fenosa, Iberdrola, Eon, Red Eléctrica de España, and Bombardier, and public bodies (the Spanish Railway Foundation, the Ministry of Public Works, and the European Commission). He has coauthored over 38 journal and conference articles and book chapters in this field.

IEEE Proof